Combination of regional and global geoid models at continental scale application to Iranian geoid

Hosseini-Asl, Mahin; Amiri-Simkooei, Alireza; Safari, Abdolreza

DOI
10.4401/AG-8643

Publication date
2021

Document Version
Final published version

Published in
Annals of Geophysics

ANNALS OF GEOPHYSICS, 64, 4, GD434, 2021; doi:10.4401/ag-8643
OPEN ACCESS

Combination of regional and global geoid models at continental scale: application to Iranian geoid

Mahin Hosseini-Asl*[,1], Alireza Amiri-Simkooei[2,3], Abdolreza Safari[1]

(1) School of Surveying and Geospatial Engineering, College of Engineering, University of Tehran, Iran
(2) Department of Geomatics Engineering, Faculty of Civil Engineering and Transportation, University of Isfahan, 81746-73441 Isfahan, Iran
(2) Department of Geoscience and Remote Sensing, Faculty of Civil Engineering and Geosciences, Delft University of Technology

Article history: received February 1, 2021; accepted May 17, 2021

Abstract

High precision geoid determination is a challenging task at the national scale. Many efforts have been conducted to determine precise geoid, locally or globally. Geoid models have different precision depending on the type of information and the strategy employed when calculating the models. This contribution addresses the challenging problem of combining different regional and global geoid models, possibly combined with the geometric geoid derived from GNSS/leveling observations. The ultimate goal of this combination is to improve the precision of the combined model. We employ fitting an appropriate geometric surface to the geoid heights and estimating its (co)variance components. The proposed functional model uses the least squares 2D bi-cubic spline approximation (LS-BICSA) theory, which approximates the geoid model using a 2D spline surface fitted to an arbitrary set of data points in the region. The spline surface consists of third-order polynomial pieces that are smoothly connected together, imposing some continuity conditions at their boundaries. In addition, the least-squares variance component estimation (LS-VCE) is used to estimate precise weights and correlation among different models. We apply this strategy to the combined adjustment of the high-degree global gravitational model EIGEN-6C4, the regional geoid model IRG2016, and the Iranian geometric geoid derived from GNSS/leveling data. The accuracy of the constructed surface is investigated with five randomly selected subsamples of check points. The optimal combination of the two geoid models along with the GNSS/leveling data shows a reduction of 21 mm (~20%) in the RMSE values of discrepancies at the check points.

Keywords: Geoid height approximation; Least squares 2D bi-cubic spline approximation; Least-squares variance component estimation; Correlation among geoid models; Combined geoid model.

1. Introduction

Precise determination of a local or global geoid is of particular importance in geodesy. There are several geoid determination methods, with different precision, depending on the available information and mathematical models used. A global gravity field model of the Earth is referred to as a Global Geopotential Model (GGM). GGMs are computed from the dedicated satellite gravity missions, CHAMP, GRACE and GOCE and terrestrial gravity and satellite altimeter measurements over the oceans. Regional geoid models are developed by combining short, medium and long wavelength components derived from a digital elevation model (DEM), terrestrial and space gravity data, low degree global geopotential models, satellite altimeter measurements, GNSS/leveling data and so on. Regional geoid computations are also based on different numerical integration of gravity anomalies, such as the integrals of Stokes, Vening-Meinesz, Poisson and Hotine [Hirt et al., 2011]. Each of the above methods has different precision due to its data requirement and computational and validation strategy.

To enhance the geoid model precision, we aim to combine different regional and global geoid models and the geometric geoid model derived from GNSS/leveling network. The global geoid models usually use the terrestrial data over the land to provide the medium wavelengths. Due to the lack of Iranian proprietary gravity and GNSS/leveling data in GGM computations, direct use of GGMs does not guarantee accurate geoid heights. Terrestrial data offer medium and short wavelength information to local and regional models. GNSS/leveling data provide the short and ultra-short wavelength components of geoid, but there may be a significant systematic effect due to the leveling network. The gravity network can also contain systematic effects over the study area. The optimal combination of different geoid models along with the elimination of their systematic effects can lead to a more reliable and precise geoid model.

The ellipsoidal height h measured by GNSS receivers, orthometric height H measured by leveling methods, and the geoid height N have a well-known geometric relation as $h - H - N = 0$ [Kotsakis and Sideris, 1999]. Many studies are ongoing on identifying appropriate functional and stochastic models to establish this relationship. Fotopoulos [2005] applied the minimum norm quadratic unbiased estimator technique, MINQUE, as the stochastic model, and various parametric surfaces, as the functional model, to the combined adjustment of geoid models and GNSS/leveling data. Their results showed that the type of parametric model affects the estimated values of variance components. In a combined least squares adjustment of ellipsoidal and orthometric heights and gravimetric geoid, Guo and Xu [2015] computed the covariance matrices of these observations. They have also used the MINQUE method to calibrate the error of their regional geoid model. Their functional model was a polynomial of order two. They also used two statistical models for validation of their results and showed the standard deviation of ~0.047 m using the priori covariance matrices and of ~0.019 m by estimating the variances. This confirmed the effectiveness of the variance components estimation (VCE) method. Eshagh and Zoghi [2016] calibrated the geoid error, computed from EGM08 over Fennoscandia. They also used the VCE method through the combined adjustments of the geoid and GNSS/leveling heights using de-trended surfaces of four, five and seven parameters. Based on the 7-parameter surface model, the average error of the EGM08 geoid became 0.048 m over the study area.

The optimal combination of different geoid models requires fitting an appropriate geometric surface to the geoid heights and estimating their (co)variance components. We need an appropriate functional model and simultaneously a realistic stochastic model to establish such an optimal combination. Both functional and stochastic models are formulated using the well-known least-squares principle.

The functional model is constructed based on the least squares 2D bi-cubic spline approximation (LS-BICSA) proposed by Amiri-Simkooei et al. [2018]. LS-BICSA, generally applicable to a set of irregular data, is formulated by the bi-cubic spline functions. The region must be divided into some patches and the patches must be connected together. This method does not necessarily require a set of grid knots or a rectangular network. Spline curve or surface fitting from scattered data sets is an active research in many fields of science and engineering.

Zhang et al. [2016] gave a thorough overview of different types of 2D spline approximations along with their basis functions. Their main difference with LS-BICSA relies on how to impose the continuity constraints. The constraints are usually imposed implicitly in the basis functions. Therefore the first, second and the higher order derivatives are automatically continuous along and across the borders. This is not the case for LS-BICSA for which the user can impose less or additional continuity constraints at the boundary knots.

The stochastic model estimates the unknown (co)variance components of observables using VCE methods. There exists a variety of VCE methods such as the minimum norm quadratic unbiased estimator (MINQUE) [Rao, 1971],

the maximum likelihood estimator (MLE) [Patterson and Thompson, 1971], the best invariant quadratic unbiased estimator (BIQUE) [Koch, 1978], the restricted maximum likelihood (REML) estimator [Koch, 1986] and the least-squares variance component estimation (LS-VCE) [Teunissen, 1988; Amiri-Simkooei, 2007]. LS-VCE is used to estimate precise weights and correlations among the models in this contribution. LS-VCE is a simple, flexible and attractive estimation principle of which we named a few. LS-VCE can determine the covariance matrix of the estimated (co)variance components. The a-priori information on the (co)variance components can simply be introduced to the stochastic model as hard/weighted constraints [Amiri-Simkooei, 2007]. The problem of negative variance components can be avoided by using the non-negative LS-VCE, which incorporates non-negativity constraints to the formulation [Amiri-Simkooei, 2016].

For the past three decades, a number of regional geoid models have been determined in Iran. The first model generated the higher order coefficients of the GPM2 geopotential model using terrestrial gravity data, based on an integral formula [Weber and Zomorrodian, 1988]. Safari et al. [2005] used the Bruns formula based on the Abel-Poisson integral. Kiamehr [2006] applied the least-squares modification of the Stokes formula. IRGeoid10 was then determined by Hatam [2010] based on the remove-restore technique along with the Stokes's formula and Helmert's second condensation method. Saadat et al. [2018] determined the regional geoid model of Iran, IRG2016, based on the radial basis functions.

Combination of regional and global geoid models, in a small-scale region in Iran, has been studied by Khazraei et al. [2017]. They used LS-VCE to evaluate the EGM2008 and GGMplus Earth geopotential models and IRGeoid10 in terms of agreement to the GNSS/leveling observations. They employed only 2D first order and second-order polynomials as a functional model, due to the small size of the study area (~100 km^2). They indicated that the second-order polynomial was superior over the first-order polynomial, and the EGM2008 gave the best results with the standard deviation of about 0.002 m, in this small-scale region. Such an issue is the subject of investigation in this paper at regional scale. Polynomials of the first and second-order are no longer effective over the large areas and the third-order spline with appropriate continuity constraints is recommended. Mosayebzadeh et al. [2019] presented the spectral improvement of the global geopotential models using regional GNSS/leveling data. The regional improvement of the global geopotential model was developed for Iran based on the EGM2008 model. The VCE method has also been applied to allocate the appropriate weights to the geoid surfaces.

The above studies estimated only the variance components but the correlations among different models were ignored. Such a stochastic model is indeed only suboptimal. It is therefore necessary to consider the correlations between different observables along with the variance components to be estimated in the stochastic model.

The remaining parts of this paper are organized as follows. In the following section, the functional model, LS-BICSA will be explained. We then briefly review LS-VCE. We apply the method to combined adjustments of the high-degree global model EIGEN-6C4, the regional geoid model IRG2016, and the geometric geoid derived from GNSS/leveling network covering Iran. Challenges for this combination will also be highlighted in this section. The regional and global geoid models and GNSS/leveling network of Iran are then introduced in a subsequent section. The resulting surface is compared with five independent data sets of GNSS/leveling check points. Finally, some conclusions are made in the last section.

2. Mathematical and statistical background

We propose the functional model, LS-BICSA, and also LS-VCE as a stochastic model. Both will be of use in a challenging problem of combining the different geoid models.

2.1 Functional model of LS-BICSA

To approximate a 2D function values using a smooth spline surface, LS-BICSA can be introduced as a reliable and flexible method [Amiri-Simkooei et al., 2018]. LS-BICSA is based on the pure bi-cubic spline functions, but in the least squares sense. It is applicable to a set of irregular data distributed in the region. The spline surface consists of third-order polynomial pieces that are smoothly connected together having some continuity conditions at their boundaries. The region must be divided into some patches and the patches must be connected to each other

longitudinally and laterally. The approximation accuracy is improved by decreasing the size of the patches. There will be 16 unknowns for each patch as a third-order polynomial. The linear model of observation equations can be formulated at the point of interest (φ, λ) as

$$N(\varphi,\lambda) = \sum_{i=0}^{3}\sum_{j=0}^{3} a_{ij}\,\varphi^i\lambda^j \tag{1}$$

where N can consists of three classes of geoid height observations corresponding to the GNSS/leveling network and those obtained from the available regional and global geoid models. Also the connecting knots must be defined by the user at the boundaries of the surface patches. We should impose that the function values, the first order derivatives, the cross derivatives and the second order derivatives are continuous at the boundary knots. To better explain the appropriate patch sizes, the required number of boundary knots and hard constraints, the reader is referred to Amiri-Simkooei et al. [2018]. The user thus may impose some hard constraints into the functional model. Considering the linear model of observations and constraint equations, we may use the following representation [Teunissen, 2000a]

$$E(y) = Ax; \qquad B^T x = 0; \qquad D(y) = Q_y \tag{2}$$

where E and D denote the mathematical expectation and dispersion operators, respectively. y is the n-dimensional vector of observations, here the same geoid height observations, x is the u-vector of the unknown parameters, A is the $n \times u$ design matrix, B is the $u \times b$ constraint matrix and Q_y is the $n \times n$ covariance matrix of observations. A and B are both assumed to be full-column rank matrices. The least squares estimate of x is $\bar{x} = B^{\perp}\,\hat{\lambda}$, where $B^{\perp}$ is the basis matrix for the null space of matrix B and $\hat{\lambda}$ is an estimated $(u - b)$-vector.

$$\hat{\lambda} = \left(B^{\perp T}A^T {Q_y}^{-1} AB^{\perp}\right)^{-1} B^{\perp T}A^T {Q_y}^{-1} y \tag{3}$$

The least squares estimate of y is $\hat{y} = {P^{\perp}}_{AB^{\perp}}\hat{\lambda}$ and $\hat{e} = {P^{\perp}}_{AB^{\perp}} y$ is the least-squares residuals. ${P^{\perp}}_{AB^{\perp}} = I_n - AB^{\perp}\left(\left(AB^{\perp}\right)^T {Q_y}^{-1} AB^{\perp}\right)^{-1}\left(AB^{\perp}\right)^T {Q_y}^{-1}$ is an orthogonal projector. Decreasing the patch size can provide smaller residuals and hence a better approximation. The least squares cubic spline approximation (LS-CSA) can also be introduced to approximate the 1D data in the least squares sense. The functional model is a piecewise cubic curve fitted to a number of consecutive data using the LS-CSA [Zangeneh-Nejad et al., 2017].

There is also an alternative functional model for LS-BICSA. When formulating a spline as a linear combination of basis functions, it is called a B-spline or Basis spline [De Boor, 1962]. B-spline automatically applies all continuity constraints, whereas LS-BICSA imposes only the user-specified constraints.

2.2 Stochastic model of LS-VCE

An appropriate stochastic model of observables leads to the best linear unbiased estimation (BLUE) of unknown parameters. The precision of the estimated parameters can be increased if the covariance matrix Q_y of observables is known. The unknown (co)variance components of Q_y can be estimated by variance component estimation (VCE). The least-squares variance component estimation (LS-VCE) is used to estimate precise weights and correlations among different observables. LS-VCE can be applied to a linear model of observation equations such as our functional model [Teunissen and Amiri-Simkooei, 2008]. We express the structure of the covariance matrix as an unknown linear combination of known cofactor matrices Q_k

$$E(y) = Ax; \qquad B^T x = 0; \qquad D(y) = Q_y = \sum_{k=1}^{p} \sigma_k Q_k, \tag{4}$$

where σ_k's are unknown (co)variance components to be estimated as $\hat{\sigma} = M^{-1} l$, where M is the $p \times p$ normal matrix, l is a $p \times 1$ vector and $\hat{\sigma} = [\hat{\sigma}_1, \cdots, \hat{\sigma}_p]^T$ is the p-vector estimated unknown (co)variances. The normal matrix M and the vector l are obtained as

$$m_{ij} = \tfrac{1}{2}\,\mathrm{tr}\left(Q_i Q_y^{-1} P^{\perp}_{AB^{\perp}} Q_j Q_y^{-1} P^{\perp}_{AB^{\perp}}\right), \qquad l_i = \tfrac{1}{2}\,\hat{e}^T Q_y^{-1} Q_i Q_y^{-1} \hat{e} \qquad i,j = 1,2,\cdots,p \tag{5}$$

Thus, if we are given the LS-BICSA functional model, along with the design and constraint matrices, A and B, the unknown covariance components can be estimated using the above equations.

2.3 Strategy to combine geoid models

Assuming a number of available geoid models, covering the study area, the goal is to obtain an appropriate geometric surface to approximate the geoid heights. This can be achieved through combining different geoid models for which the functional and stochastic models of geoid heights must be well defined. LS-BICSA and LS-VCE will be used as the functional and stochastic models, respectively. LS-VCE describes the statistical properties of different geoid models by means of the covariance matrix. We use this procedure through combined adjustments of two geoid models EIGEN-6C4 and IRG2016 and also GNSS/leveling geoid heights, covering Iran. For the sake of comparison, three scenarios are proposed based on the combination of different observations along with their different statistical properties.

- **Scenario I**

  Scenario I provides a combination of two geoid models EIGEN-6C4 and IRG2016, solving for the functional model LS-BICSA, using only the initial covariance matrices. Because the initial covariance matrix of the global model is available, and that of the regional model is not, the covariance matrices are considered as the identity matrix. Therefore, under scenario I, the two models are equally weighted.

- **Scenario II**

  In scenario II, the variance components of two geoid models EIGEN-6C4 and IRG2016, are considered to be unknown and therefore they are estimated by LS-VCE. The covariance components among the geoid models can also be considered unknown. The stochastic model of the different geoid height data sets then reads (see Eq. 4)

$$Q_y = \sigma^2_{EIG} Q_{EIG} + \sigma^2_{IRG} Q_{IRG} + \sigma_{EIG,IRG} Q_{EIG,IRG} \tag{6}$$

  where σ^2_{EIG}, σ^2_{IRG} and $\sigma_{EIG,IRG}$ are the unknown variances and covariance between the two geoid models, respectively. The initial information about the covariance matrices can simply be introduced to the stochastic model when using LS-VCE. The correlation coefficient between the two models is also obtained by

$$\rho_{EIG,IRG} = \frac{\sigma_{EIG,IRG}}{\sqrt{\sigma^2_{EIG}}\sqrt{\sigma^2_{IRG}}} \tag{7}$$

- **Scenario III**

  In principle, the accuracy of the calculated geoid is usually assessed by comparing it with the geoid heights derived from GNSS/leveling. But, as an alternative, it is suggested to combine the GNSS/leveling data to further enhance the accuracy of the combined model. Scenario III provides such a combination. The stochastic model of this scenario is then given as

$$Q_y = \sigma^2_{EIG} Q_{EIG} + \sigma^2_{IRG} Q_{IRG} + \sigma^2_{G/L} Q_{G/L} + \sigma_{EIG,IRG} Q_{EIG,IRG} \tag{8}$$

  where $\sigma^2_{G/L}$ is the unknown variance component of the geoid height derived from GNSS/leveling.

Four unknown variance and covariance components are estimated by LS-VCE. Scenario III was performed once using the existing 1288 GNSS/leveling points, and once the outliers were identified by the Baarda's data-snooping algorithm at the 99% confidence level [Baarda, 1968; Teunissen, 2000]. Under such a condition, a number of GNSS/leveling points were identified as outliers, and therefore left out from the process.

To evaluate the estimated models, independent check points are needed. We applied the cross-validation method to reduce the impact of the control point's distribution on the results and evaluations. Cross validation is often used to show the stability of a model with respect to different distributions of check points [Gholinejad et al., 2019]. The accuracy of the constructed surfaces is investigated with five randomly selected subsamples of such check points.

Because the estimation in the stochastic model is an iterative process, one needs to define the initial values for the unknown parameters and a threshold limit to stop the iterations. The initial values of the variance and covariance components are assumed to be equal to 1 and 0, respectively, and the threshold value is set to $\varepsilon = 10^{-8}$. We noted that increasing the number of model combinations and therefore dealing with a large amount of observations, constraints and unknowns makes it difficult to calculate in both functional and stochastic models. One may then optimize the computational time and memory usage by employing structured data sets. Such an algorithm, presented by Amiri-Simkooei [2009], uses some operators and assumptions to come-up with a computationally less-expensive solution in the functional and stochastic models.

3. Available geoid models

The aim of this study is to combine different geoid models, based on the least-squares adjustment of functional and stochastic models, i.e. LS-BICSA and LS-VCE. The study area is limited between the latitudes of 25.18° N and 40° N and longitudes of 44° E and 63° E. We will introduce the geoid models, as well as the available GNSS/leveling control points over the area of interest.

3.1 Global Geopotential Model

The global geoid models are typically expressed as a set of spherical harmonic coefficients, derived from satellite measurements, and terrestrial and altimetry gravity data. Therefore, the geoid height can be determined in spherical approximation from the coefficients of any gravity field model [Heiskanen and Moritz, 1967]. These GGM geopotential coefficients can be obtained from the ICGEM database at GFZ Potsdam via http://icgem.gfz-potsdam.de. Because the standard deviation of the spherical harmonic coefficients is also given by the global models, the geoid height variances and thus the covariance matrix of observables can be calculated.

Two extra-high spherical harmonic models, EGM2008 and EIGEN-6C4 have been used in parallel in recent studies over the Iranian territory. The brief description of these models is provided in Table 1. EIGEN-6C4 is computed from more data sources than EGM2008, according to Table 1. Ebadi et al. [2019] showed that the results based on EGM2008 are generally close to those of EIGEN-6C4 in their numerical analyses. Foroughi et al. [2017] indicated that EIGEN-6C4 achieves the lowest root mean square error (RMSE) value for estimating the geoid heights, whereas EGM2008 provides the closest results to the terrestrial gravity anomalies over Iran. Saadat et al. [2018] showed that EIGEN-6C4 has the minimum RMSE value for the difference in geoid height at 1288 GNSS/leveling control points over Iran. We therefore preferred EIGEN-6C4 for all numerical analyses. The geoid height of the model was computed in terms of a resolution 5-arcmin grid, covering the study area, with reference to the WGS84 ellipsoid.

Models	Year	Deg.	Satellite Data	Surface Data	References
EGM2008	2008	2190	GRACE	DNSC07 Altimetry SS v18.1 Altimetry NGA08 Land	Pavlis et al. [2012]
EIGEN-6C4	2014	2190	GRACE, GOCE, LAGEOS	DTU10 Altimetry EGM2008 Land	Förste et al. [2014]

Table 1. Global geopotential models

3.2 Regional geopotential model

Along with the global model, the Iranian gravimetric geoid IRG2016 has also been used in this contribution. IRG2016 is based on the radial basis functions (RBFs) and is limited between 25° N and 40° N in latitude and 44° E and 63.5° E in longitude [Saadat et al., 2018]. IRG2016 uses the data sets of 21525 gravity data provided by NCC of Iran. Residual gravity disturbances were computed by subtracting the EIGEN-6C4 model up to degree 360 and applied to determine the unknown RBF parameters by the stabilized orthogonal matching pursuit (SOMP) algorithm. The model was fitted to GNSS/leveling control points by applying the 6 parameter polynomial surface. The results show an RMSE value of approximately 0.23 m for the difference in geoid height. The accuracy of the resulting geoid was strongly dependent on the accuracy and distribution of the gravity data over the area of interest. Saadat et al. [2018] showed also the large gaps located in the south-east of the country and the Lut and Kavir central desert of Iran. The gridded 2.5-arcmin model is on-demand available at the International Service for the Geoid (ISG) website, while the model interpolation can be performed by http://www.irg2016.ir.

3.3 GNSS/leveling network

The accuracy of the calculated geoid models is usually evaluated in scattered control points within the study area. The best and most reliable way to estimate the deviations of a gravimetric geoid model is to use the GNSS/leveling network. The GNSS/leveling network of Iran consists of 1288 stations where their orthometric heights are connected to the Iranian precise leveling network using the DN-G1001 benchmark, located in the southern part of the country. The precise geodetic height and horizontal position of the stations was measured by the Dual-frequency GNSS receivers and the observations were transformed to the original version of WGS84 coordinate system, known as the Iranian Geodetic Datum IRGD2010.

There can be a significant systematic effect across the country due to the leveling network. The Iranian height datum is only tied to a single tide-gauge station DN-G1001. The other biases can also occur for a variety of reasons, such as theoretical approximations made in processing observed data and network adjustments, approximate or inexact normal/orthometric height corrections, instability of reference station monuments over time and so on [Fotopoulos, 2005]. On the other hand, the regional model can contain systematic effects over the study area. There are also datum inconsistencies inherent among the geoid models. We have used the 3D affine transformation to minimize the possible systematic effect of the GNSS/leveling network and the regional model, compared to the EIGEN-6C4. The distribution of the GNSS/leveling network and their geoid heights after 3D affine transformation have been shown in Figure 1. Figure 2 shows the residuals of IRG2016 geoid height from EIGEN-6C4 after 3D affine transformation.

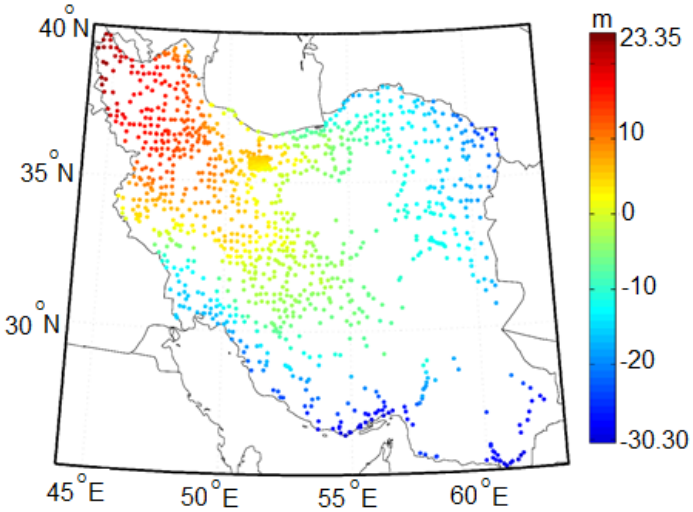

Figure 1. Distribution of 1288 GNSS/leveling control points and their geoid heights over Iran.

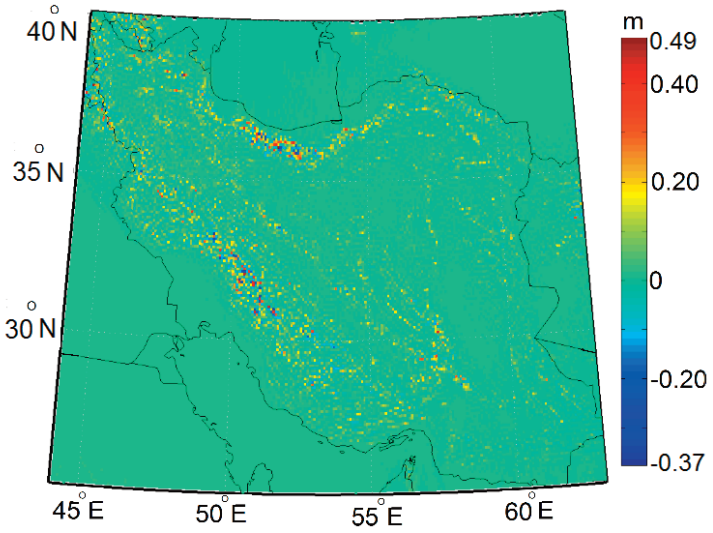

Figure 2. The difference in geoid heights between EIGEN-6C4 and IRG2016.

4. Numerical results and discussions

The accuracy of the available geoid models and also the performance of the proposed functional model was assessed at the start of this section. The geoid heights of the two models, EIGEN-6C4 and IRG2016, are generated at a grid with 5-arcmin spacing after applying the 3D transformation. Each geoid model is separately approximated by LS-BICSA and a few 2D polynomials such as the first-order bi-linear, the second-order bi-quadratic and the third-order bi-cubic polynomials with four, nine and 16 unknown coefficients, respectively. These polynomials approximate the geoid surfaces over the study area. To define the LS-BICSA, the splines are considered with 10-arcmin patch sizes and these patches are connected together at four boundary knots, longitudinally and laterally. As the study area is limited between the latitudes of 25.18° N and 40° N and longitudes of 44° E and 63° E, the entire region is divided into 89×114 surface patches. The comparison of these models with GNSS/leveling control points is given in Table 2. The geoid height differences showed that the 2D polynomials cannot appropriately approximate such a large region. But the geoid of the region is well approximated using LS-BICSA.

Models	Approximation method	Min	Max	RMSE
EIGEN-6C4	Bi-linear	-9.699	8.1656	2.888
	Bi-quadratic	-15.608	11.736	3.446
	Bi-cubic	-10.644	6.927	2.923
	LS-BICSA method	-0.425	0.433	0.155
IRG2016	Bi-linear	-9.157	7.621	2.835
	Bi-quadratic	-14.811	10.966	3.412
	Bi-cubic	-10.251	6.453	2.909
	LS-BICSA method	-0.402	0.418	0.142

Table 2. Geoid height differences at GNSS/leveling points, after 3D affine transformation and data-snooping. Units in meters.

4.1 Implementation on three scenarios

To perform the combination, geoid heights of two models, EIGEN-6C4 and IRG2016 and also the geoid heights derived from GNSS/leveling network are provided after applying the 3D transformation. As mentioned, three scenarios were considered. Scenario I provides a combination of two geoid models, solving for the functional model and using the initial variance-covariance matrices. Figure 3 shows the difference between the estimated surface in scenario I and both the EIGEN-6C4 and IRG2016. In the second scenario, the variance components of the geoid models are considered unknown and are to be estimated by LS-VCE. All variance and covariance components among the models along with the new estimated surface are obtained in this scenario. Figure 4 shows the difference between the estimated surface and EIGEN-6C4 and IRG2016, under scenario II.

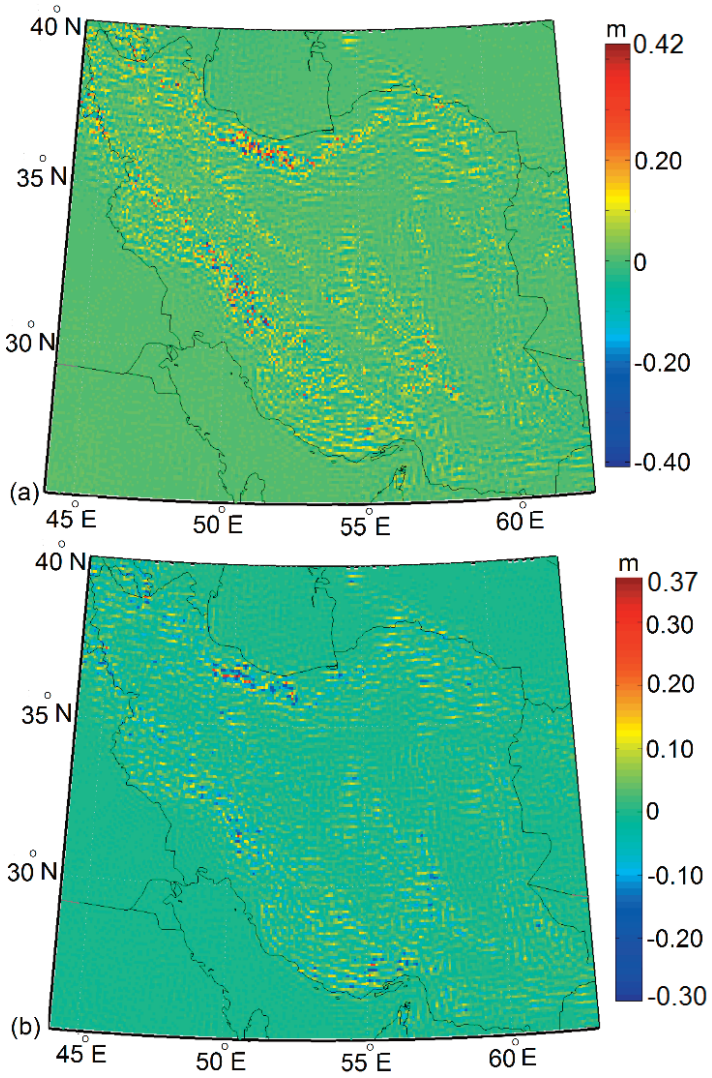

Figure 3. The difference between the estimated surface and (a) EIGEN-6C4 and (b) IRG2016, in scenario I.

Figures 3 and 4 show that the estimated residuals of the regional model are smaller than the global model due to the use of the terrestrial gravity data in the regional model generation. On the other hand, neglecting the (co)variance components, as we do in scenario I, gives identical weights to the global and regional models. But scenario II provides more realistic results, because it takes into consideration the (co)variances among the models.

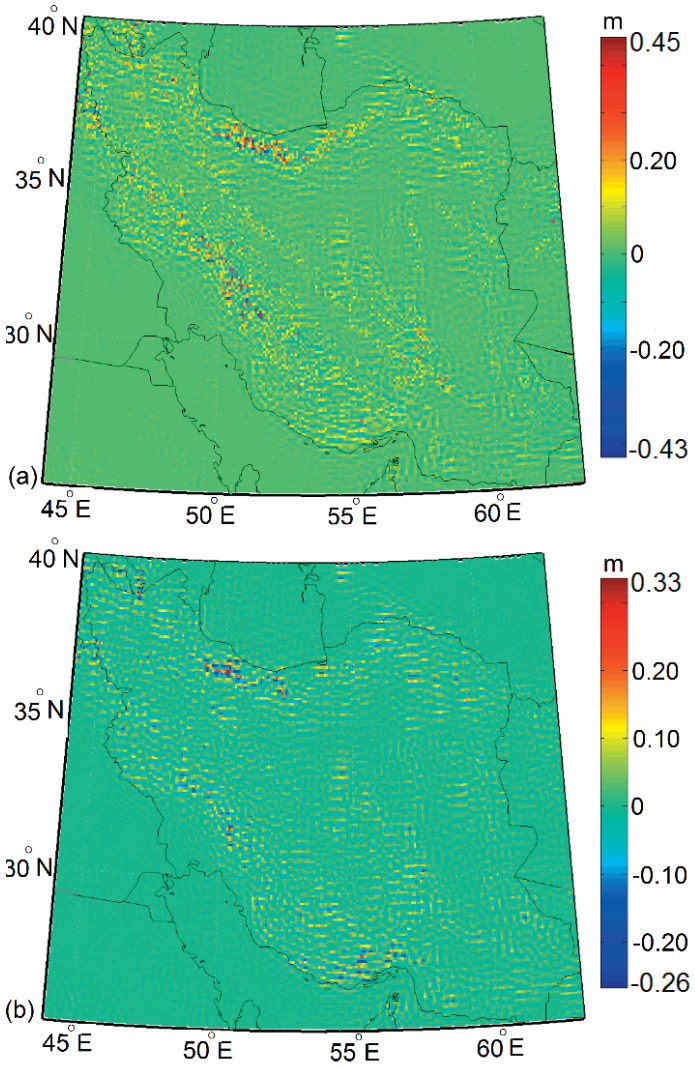

Figure 4. The difference between the estimated surface and (a) EIGEN-6C4 and (b) IRG2016, in scenario II.

Under this scenario, the estimated surface becomes closer to the regional model (see later on). Therefore estimating the optimal weight of observations can have significant effect on estimating the geoid surface. Figure 5 shows the difference between the estimated surfaces under scenarios I and II.

Finally, scenario III provides a combination of the two geoid models and the geoid heights derived from GNSS/leveling data. The unknown (co)variance parameters can also be estimated for each model from Eq. (8). Table 3 presents the value of the estimated standard deviations of geoid models and the correlation coefficients under scenario II and scenario III. The standard error of the regional model is smaller than the global model in both scenarios, in agreement with the results in Figure 4. On the other hand, the geoid derived from GNSS/leveling data has the standard error of 0.117 m. The low-density and inhomogeneous distribution of the GNSS/leveling points over Iran, errors in observations, the lack of simultaneity of GNSS and leveling observations and crust, earthquakes, land subsidence phenomenon are some factors that can reduce the GNSS/leveling accuracy.

Scenario	σ_{EIGEN} (m)	$\sigma_{IRGeoid16}$ (m)	$\sigma_{GNSS/L}$ (m)	$\hat{\rho}_{EIGEN,IRG\ 2016}$
II	0.064	0.055	_	0.64
III	0.072	0.061	0.117	0.63

Table 3. Estimated standard deviation and correlation of geoid models in scenarios II and III.

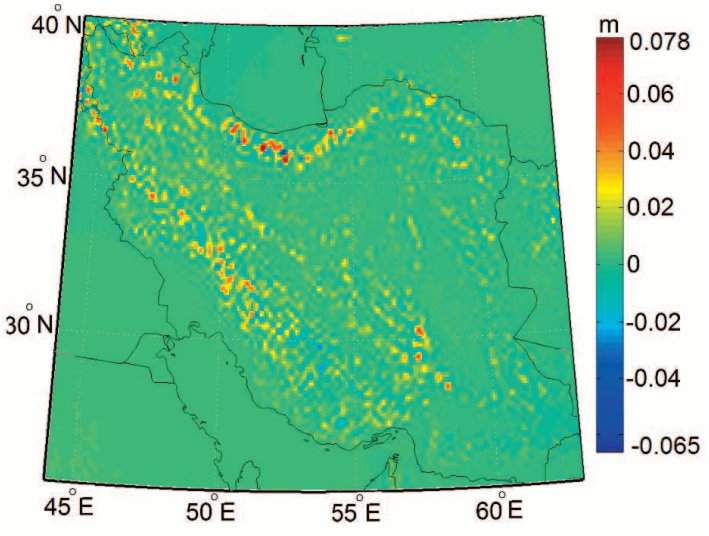

Figure 5. The difference between the estimated surfaces under scenario I and II.

Table 3 also shows the correlation coefficient of about 0.63 between the two models. This makes sense because the EIGEN-6C4 is used in the long wavelengths of the IRG2016 in the model generation. Figure 6 shows the difference between the estimated surface and the EIGEN-6C4 and IRG2016 geoid models in scenario III. Smaller residuals in Figure 6b indicate that IRG2016 is closer to the combined model. Figure 7 also shows the difference between the estimated surfaces under scenarios II and III. This indicates that GNSS/leveling has significant contribution in the construction of the combined geoid model.

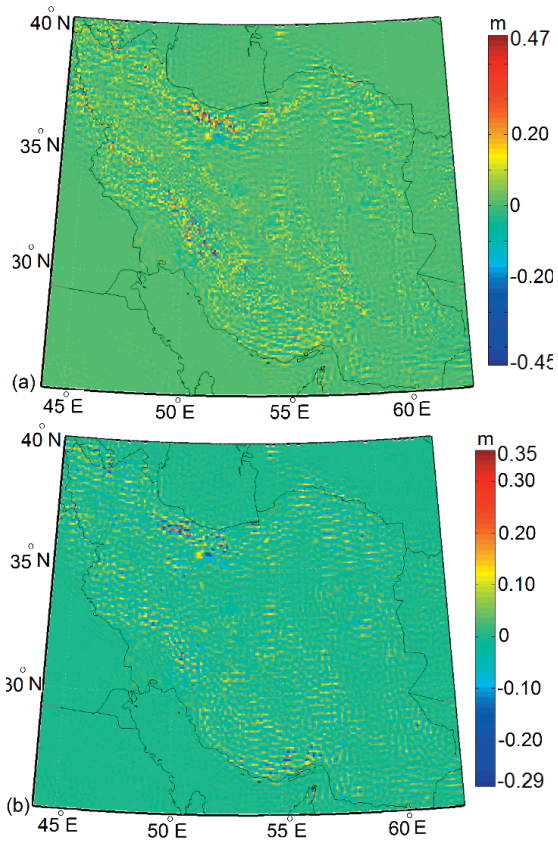

Figure 6. The difference between the estimated surface and (a) EIGEN-6C4 (b) IRG2016 in scenario III.

Five data sets of check points were selected randomly to cross-validate the results. For each test, 130 GNSS/leveling points were introduced as the check points, indicating that they had no contribution to the (co)variance components. These randomly selected subsamples of GNSS/leveling network follow a uniform distribution over the study area. The remaining points of the GNSS/leveling network participate in the scenario III as the observation data set. Figure 8 shows the randomly distributed check points and also observation points in data set 1. As can be seen, both check and observation collections are extended in the same study area. Thus scenario III was implemented five times for the five different observation sets. The RMSE of each scenario is calculated related to five data sets and then the average RMSE is considered as the final RMSE for comparison. Table 4 provides some statistics of the geoid height differences in scenarios I, II and III compared with the GNSS/leveling data sets. Since the regional model and GNSS/leveling data have been transferred to the EIGEN-6C4 by 3D affine transformation, the differences are zero-mean. Then the RMSEs and standard deviations are the same, which is not presented in Table 4.

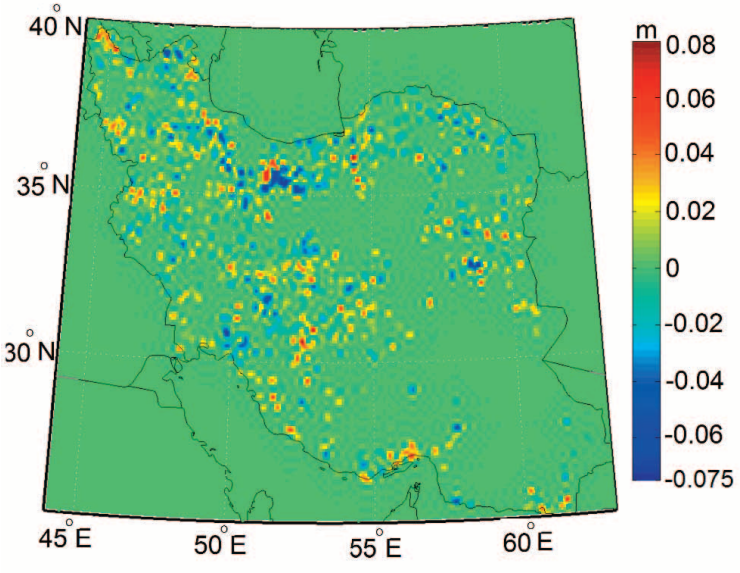

Figure 7. The difference between the estimated surface under scenario II and III.

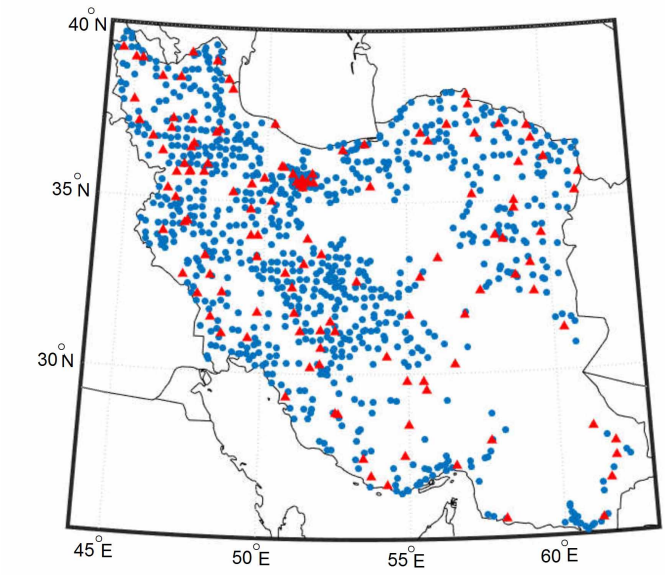

Figure 8. GNSS/leveling points used for development of scenario III (dots) and 130 GNSS/leveling checkpoints (triangles), data set 1.

Set	EIGEN-6C4			IRG2016			APRX (scen I)			APRX (scen II)			APRX (scen III)		
	min	max	RMS	min	Max	RMS	min	max	RMS	min	max	RMS	min	max	RMS
1	-0.392	0.372	0.143	-0.359	0.351	0.133	-0.343	0.336	0.130	-0.316	0.313	0.125	-0.263	0.267	0.113
2	-0.405	0.382	0.147	-0.370	0.361	0.138	-0.350	0.345	0.135	-0.323	0.321	0.129	-0.279	0.271	0.116
3	-0.395	0.379	0.142	-0.363	0.354	0.136	-0.348	0.337	0.131	-0.318	0.315	0.126	-0.276	0.268	0.114
4	-0.401	0.381	0.144	-0.364	0.351	0.135	-0.353	0.340	0.132	-0.325	0.320	0.126	-0.285	0.272	0.115
5	-0.380	0.383	0.144	-0.365	0.360	0.136	-0.352	0.342	0.131	-0.325	0.318	0.128	-0.271	0.277	0.115
Ave.	-0.394	0.379	0.144	-0.364	0.355	0.135	-0.349	0.340	0.131	-0.321	0.317	0.126	-0.274	0.270	0.114

Table 4. RMSE, min and max values of geoid height differences at five sets of check points for EIGEN-6C4, IRG2016 and three scenarios of their combinations. Units in meters.

IRG2016 gives better results than EIGEN-6C4 in terms of RMSE value in each data set. This is in agreement with the results provided in Table 3, which provides the minimum standard deviation for this model under scenarios II and III. The results also indicate that the approximated surface in scenario I has the maximum height difference and RMSE values of 0.349 m and 0.131 m, respectively. Therefore, this scenario does not provide realistic results because it ignores the optimal (co)variance components. The results under scenario II contain smaller geoid height differences than scenario I. The maximum height difference and RMSE values of this scenario reach 0.321 m and 0.126 m. It further confirms that the optimal combination of available geoid models, including appropriate functional and stochastic models, can improve the height reference surface. Scenario III gives the superior results in terms of RMSE value among the existing scenarios. The combination of the GNSS/leveling data with the regional and global models led to an improvement of the RMSE value to 0.114 m. The maximum height difference is also about 0.277 m in this scenario. Figure 9 shows the height differences between the estimated surface under three scenarios and GNSS/leveling check points in data set 1. In conclusion, such a combination of all available data sets can result in an appropriate geometric model over the study area. However the low-density and inhomogeneous distribution of the GNSS/leveling data can reduce the assessment accuracy.

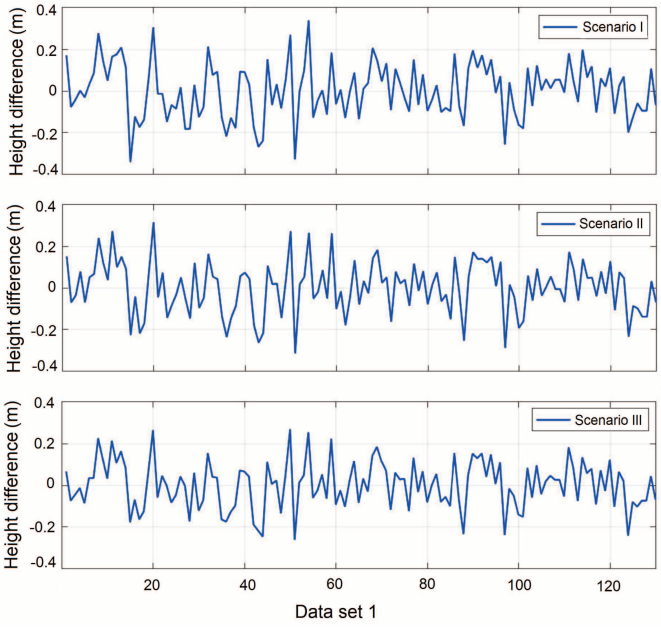

Figure 9. The height differences between the estimated surface under three scenarios and check points in data set 1.

The assessment will further be degraded due to the lack of simultaneity of GNSS and leveling observations as substantial unmodeled land subsidence has occurred in different parts of the study area. The estimated surface under scenario III is shown in Figure 10.

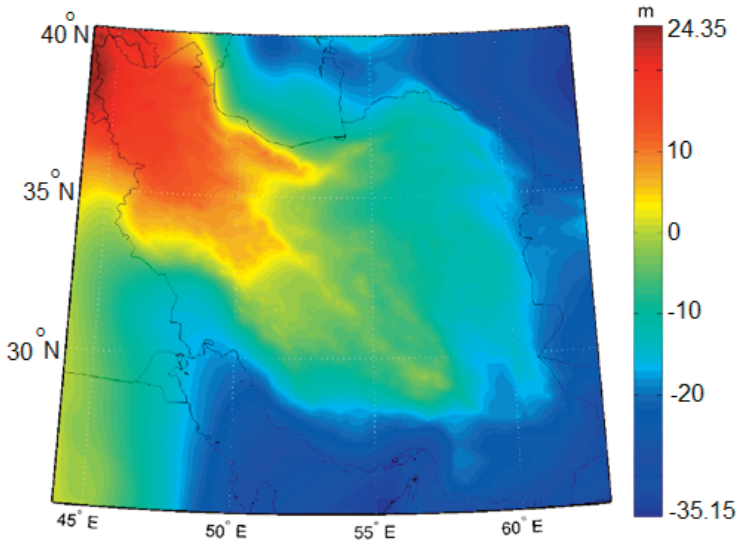

Figure 10. Approximated surface under scenario III.

5. Conclusions

The aim of this study was to present a strategy to combine different geoid models using a smooth surface. In this contribution, LS-BICSA and LS-VCE methods were introduced to build the functional and stochastic models. To investigate the performance of the method, the results of three scenarios were presented and five data sets of GNSS/leveling check points were selected to cross-validate the results. The first scenario did not consider the optimal weights and therefore did not significantly improve the results. (Co)variance components estimation, LS-VCE, led to increasing the precision of approximated surface in scenario II. Finally, by including the GNSS/leveling observations in scenario III, the mean RMSE value on check points reduces and this optimal combination was shown to have the best performance.

In conclusion, the optimal combination of different geoid models along with the elimination of systematic effects can lead to a more reliable geoid. The biases were eliminated before we use them in the combination. The approximated surface is strongly dependent on the accuracy of the geoid models used. On the other hand, the accuracy assessment depends largely on the accuracy of the available GNSS/leveling control points. The low-density of the control points, the lack of simultaneity of GNSS and leveling observations and land subsidence phenomenon can reduce the accuracy assessment. The subsidence phenomenon is noticed to take place in many areas of Iran and thus such control points require permanent maintenance and periodic re-measurements. If such a clean GNSS/leveling data set becomes available in the future, they can be introduced to the LS-VCE as a constrained model, leading to a further improvement of the approximated model.

Data availability. Some data used during the study were provided by a third party (GNSS/leveling heights were provided by the National Cartographic Center (NCC) of Iran). Direct request for these materials may be made to the provider as indicated in the Acknowledgments. Some or all data, models, or code that support the findings of this study are also available from the corresponding author upon reasonable request (Regional geopotential models and all related code used to analyze data).

Acknowledgments. We would like to acknowledge the National Cartographic Center of Iran for providing us with the GNSS/leveling control stations used in this research.

References

Amiri-Simkooei, A.R. (2007). Least-squares variance component estimation: theory and GPS applications, PhD thesis, Delft University of Technology, Netherlands.

Amiri-Simkooei, A.R. (2009). Noise in multivariate GPS position time series, J. Geod., 83, 175–187, https://doi.org/10.1007/s00190-008-0251-8.

Amiri-Simkooei, A.R. (2016). Non-negative least-squares variance component estimation with application to GPS time series, J. Geod., 90, 5, 451–466, https://doi.org/10.1007/s00190-016-0886-9.

Amiri-Simkooei, A.R., M. Hosseini-Asl and A. Safari (2018). Least squares 2D bi-cubic spline approximation: Theory and Applications, Measurement, 127, 366-378, https://doi.org/10.1016/j.measurement.2018.06.005.

Baarda, W. (1968). A testing procedure for use in geodetic networks, Netherlands Geodetic Commission, Publication on Geodesy, New Series, 2, 5, Delft, The Netherlands.

De Boor, C. (1962). Bicubic spline interpolation, J. Math. Phys., 41, 212-218, https://doi.org/10.1002/sapm1962411212.

Ebadi, A., A.A. Ardalan and R. Karimi (2019). The Iranian height datum offset from the GBVP solution and spirit-leveling/gravimetry data, J. Geod., 93, 1207–1225, https://doi.org/10.1007/s00190-019-01237-x.

Eshagh, M., S. Zoghi, (2016). Local error calibration of EGM08 geoid using GNSS/levelling data, J. Appl. Geophys., 130, 209–217, https://doi.org/10.1016/j.jappgeo.2016.05.002

Foroughi, I., Y. Afrasteh, S. Ramouz and A. Safari (2017). Local evaluation of Earth Gravitational Models, case study: Iran, Geodesy and Cartography, 43, 1, 1-13, https://doi.org/10.3846/20296991.2017.1299839.

Förste, Ch., S.L. Bruinsma, O. Abrikosov, J.M. Lemoine, T. Schaller, H.J. Götze, J. Ebbing, J.C. Marty, F. Flechtner, G. Balmino and R. Biancale (2014). EIGEN-6C4 The latest combined global gravity field model including GOCE data up to degree and order 2190 of GFZ Potsdam and GRGS Toulouse, GFZ Data Services, http://doi.org/10.5880/icgem.2015.1.

Fotopoulos, G. (2005). Calibration of geoid error models via a combined adjustment of ellipsoidal, orthometric and gravimetric geoid height data, J. Geod., 79, 1–3, 111–123, https://doi.org/10.1007/s00190-005-0449-y.

Gholinejad, S., A.A. Naeini and A.R. Amiri-Simkooei (2019). Robust Particle Swarm Optimization of RFMs for High-Resolution Satellite Images Based on K-Fold Cross-Validation, IEEE Journal of Selected Topics in Applied Earth Observations and Remote Sensing, 12, 2594-2599, https://doi.org/10.1109/JSTARS.2018.2881382.

Guo, D.M. and Xu H.Z. (2015). Application of variance components estimation to calibrate geoid error models, SpringerPlus, 4, 434, https://doi.org/10.1186/s40064-015-1210-5.

Hatam, C.Y. (2010). Etablissement des nouveaux reseaux multi-observations geodesiques et gravimetriques et determination du geoide en Iran, PhD thesis, University Montpellier, France.

Heiskanen, W.A. and H. Moritz (1967). Physical Geodesy, WH Freeman and Company, San Francisco.

Hirt, C., W.E. Featherstone and S.J. Claessens (2011). On the accurate numerical evaluation of geodetic convolution integrals, J. Geod., 85, 8, 519-538, https://doi.org/10.1007/s00190-011-0451-5.

Khazraei, S.M., V. Nafisi, A.R. Amiri-Simkooei and J. Asgari (2017). Combination of GPS and Leveling Observations and Geoid Models Using Least-Squares Variance Component Estimation, J. Surv. Eng., 143, 2, 04016023, https://doi.org/10.1061/(ASCE)SU.1943-5428.0000205.

Kiamehr, R. (2006). Precise Gravimetric Geoid Model for Iran Based on GRACE and SRTM Data and the Least-Squares Modification of Stokes' Formula: with Some Geodynamic Interpretations, PhD thesis, Royal Institute of Technology, Sweden.

Koch, K.R. (1978). Schätzung von varianzkomponenten. Allgemeine Vermessungs-Nachrichten, 85, 264–269.

Koch, K.R. (1986). Maximum likelihood estimate of variance components, Bull. Geodesique, 60, 4, 329–338, https://doi.org/10.1007/BF02522340.

Kotsakis, C. and M.G. Sideris (1999). On the adjustment of combined GPS/levelling/geoid networks, J. Geod., 7, 8, 412–421, https://doi.org/10.1007/s001900050261.

Mosayebzadeh, M., A.A. Ardalan and R. Karimi (2019). Regional improvement of global geopotential models using

GPS/Leveling data. Stud, Geophys. Geod., 63, 169-190, https://doi.org/10.1007/s11200-017-1084-9.

Patterson, H.D. and R. Thompson (1971). Recovery of inter-block information when block sizes are unequal, Biometrika, 58, 3, 545-554, https://doi.org/10.2307/2334389.

Pavlis, N.K., S.A. Holmes, S.C. Kenyon and J.K. Factor (2012). The development and evaluation of the Earth Gravitational Model 2008 (EGM2008), J. Geophys., Res, 117, B04406, https://doi.org/10.1029/2011JB008916.

Rao, C.R. (1971). Estimation of variance and covariance components - MINQUE theory, J. Multivar. Anal., 1, 3, 257–275, https://doi.org/10.1016/0047-259X(71)90001-7.

Saadat, A., A. Safari and D. Needell (2018). IRG2016: RBF-based regional geoid model of Iran, Studia Geophys. et Geod., 62, 3, 380-407, https://doi.org/10.1007/s11200-016-0679x.

Safari, A., A.A. Ardalan and E.W. Grafarend (2005). A new ellipsoidal gravimetric, satellite altimetry and astronomic boundary value problem, a case study: The geoid of Iran, J. Geodyn., 39, 5, 545-568, https://doi.org/10.1016/j.jog.2005.04.009.

Teunissen, P.J.G. (1988). Towards a least-squares framework for adjusting and testing of both functional and stochastic model. Internal research memo, Geodetic Computing Centre, Delft, A reprint of original 1988 report is also available in 2004, 26, http://www.lr.tudelft.nl/mgp.

Teunissen, P. J. G. (2000). Testing Theory: an introduction, Website: http://www.vssd.nl: Delft University Press. Series on Mathematical Geodesy and Positioning.

Teunissen, P.J.G. (2000a). Adjustment theory: an introduction, Series on Mathematical Geodesy and Positioning, Delft University Press. hhttp://www.vssd.nli (Dec. 15, 2010).

Teunissen P.J.G. and Amiri-Simkooei A.R., (2008). Least-squares variance component estimation, J. Geod., 82, 2, 65–82, https://doi.org/10.1007/s00190-007-0157-x.

Weber, G. and H. Zomorrodian (1988). Regional geopotential model improvement for the Iranian geoid determination, Bull. Geodesique, 62, 2, 125–141, https://doi.org/10.1007/BF02519221.

Zangeneh-Nejad, F., A.R. Amiri-Simkooei, M.A. Sharifi and J. Asgari (2017). Cycle slip detection and repair of undifferenced single-frequency GPS carrier phase observations, GPS Solut., 21, 4, 1593–1603. https://doi.org/10.1007/s10291-017-0633-6.

Zhang, Y., J. Cao, Zh. Chen, X. Li and X.M. Zeng (2016). B-spline surface fitting with knot position optimization. Comput. Graph., 58,73-83, https://doi.org/10.1016/j.cag.2016.05.010.

***CORRESPONDING AUTHOR: Mahin HOSSEINI-ASL**,
School of Surveying and Geospatial Engineering,
College of Engineering, University of Tehran, Iran,
e-mail: mahin.hosseiniasl@ut.ac.ir